BOLETIN DE LA SOCIEDAD ESPAÑOLA DE
Cerámica y Vidrio
www.elsevier.es/bsecv

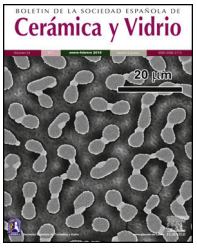

Microstructure and properties of YSZ-Al_2O_3 functional ceramic thermal barrier coatings for military applications

Mari Ramesh[a], *Krishnaswamy Marimuthu*[b], *Palanisamy Karuppuswamy*[a], *LakshmiNarasimhan Rajeshkumar*[c,*]

[a] *Department of Mechanical Engineering, Sri Ramakrishna Engineering College, Coimbatore, 641022 TN, India*
[b] *Department of Mechanical Engineering, Coimbatore Institute of Technology, Coimbatore, 641014 TN, India*
[c] *Department of Mechanical Engineering, KPR Institute of Engineering and Technology, Coimbatore, 641407 TN, India*

ARTICLE INFO

Article history:
Received 28 September 2020
Accepted 8 June 2021
Available online 29 June 2021

Keywords:
Thermal barrier coating
Yttria Stabilized Zirconia
Alumina
Atmospheric plasma spray
Thermal testing
Wear and scratch tests

ABSTRACT

Current study renders its focus on the investigation of functionally graded Yttria Stabilized Zirconia (YSZ) and alumina (Al_2O_3) thermal barrier coatings (TBC) deposited on EN steel substrates used in gun barrel through atmospheric plasma spray (APS) process. A bond coat and the top coats was made with two distinct compositions using YSZ-Al_2O_3 in 75:25 and 50:50 weight ratio through APS process with two carrier gas concentrations of 3 and 4 standard cubic feet per hour (scfh). Coatings were characterized with thermal testing, X-ray Diffraction (XRD) and Field Emission Scanning Electron Microscope examination (FESEM). Surface roughness test, wear and scratch test of the uncoated and coated steel specimens was also measured. YSZ-Al_2O_3 coated EN36C steel possessed greater insulation performance under a carrier gas flow rate of 3 scfh compared to all other specimens. EN36C steel coated with YSZ-Al_2O_3 in the ratio of 75:25 has better wear and scratch resistance indicating lesser deformation compared to other materials.

Microestructura y propiedades de los recubrimientos de barrera térmica cerámica funcional YSZ-Al_2O_3 para aplicaciones militares

Palabras clave:
Recubrimiento de barrera térmica
Zirconia estabilizada con itria
Alúmina
Spray de plasma atmosférico
Pruebas térmicas
Pruebas de desgaste y rayado

RESUMEN

El estudio actual se centra en la investigación de recubrimientos de barrera térmica (TBC) de zirconia estabilizada con itria (YSZ) y alúmina (Al_2O_3) de grado funcional depositados en sustratos de acero EN utilizados en el cañón de la pistola a través del proceso de pulverización de plasma atmosférico (APS). Se preparó una capa adhesiva y las capas superiores con dos composiciones distintas usando YSZ-Al_2O_3 en una relación en peso de 75:25 y 50:50 mediante el proceso APS con dos concentraciones de gas portador de 3 y 4 scfh. Los recubrimientos se caracterizaron con pruebas térmicas, difracción de rayos X (XRD) y examen de microscopio

* *Corresponding author.*
E-mail address: lrkln27@gmail.com (L. Rajeshkumar).
https://doi.org/10.1016/j.bsecv.2021.06.004

electrónico de barrido de emisión de campo (FESEM). También se midió la prueba de rugosidad de la superficie, la prueba de desgaste y rayado de las muestras de acero revestidas y sin revestir. El acero EN36C recubierto de YSZ-Al_2O_3 poseía un mayor rendimiento de aislamiento bajo un caudal de gas portador de 3 scfh en comparación con todas las demás muestras. El acero EN36C recubierto con YSZ-Al_2O_3 en una proporción de 75:25 tiene una mejor resistencia al desgaste y al rayado, lo que indica una menor deformación en comparación con otros materiales.

Introduction

Thermal barrier coatings (TBCs) are extensively employed in elevated temperature applications to enhance thermal insulation capability and longevity. TBCs usually comprises 6 to 8 wt.% YSZ owing to the better thermal expansion coefficient of the material, low thermal conductivity and longevity at temperatures lower than 1200 °C. Several researchers pointed that YSZ and Al_2O_3 coatings have greater potency for development of TBCs possessing lower thermal conductivities. These TBCs (100–250 μm) provides insulation to the parts to withstand large and prolonged heat loads. Large numbers of researchers are focusing on establishing new TBC systems with better thermal stability [1]. These TBCs can be utilized in defense applications for better performance and lifetime of the component. YSZ is the most commonly used material during TBCs in gas turbine and diesel engine applications. Besides this, by using plasma spraying method, only YSZ could be coated with large thickness when compared with other refractory oxide materials. YSZ is characterized by high thermal shock resistance, high coefficient of thermal expansion (CTE) and low thermal conductivity and alongside its phase instability and corrosion prone owing to exposure to oxygen, YSZ has a limited temperature working range of 1200°. On the other hand, α-Al_2O_3 is the most stable oxide among various class of alumina. Because of its chemical inertness and high hardness it becomes a potential additional coating material in any TBC application. It is also characterized with few demerits like low CTE and high thermal conductivity [2]. When Al_2O_3 is additionally coated with YSZ in TBC, bonding strength, hardness, corrosion and oxidation resistance of the coating will be greatly enhanced for almost the same toughness and elastic modulus of the material coated with YSZ alone. When compared with individual YSZ coatings, functionally graded YSZ-Al_2O_3 coatings are proven to be thermally stable coatings. Stability of individual YSZ coatings becomes questionable when the raise in temperature of coated material removes the yttrium partially from the zirconium oxide and results in formation monoclinic zirconia (m-ZrO_2) from metastable tetragonal zirconia (t'-ZrO_2) due to martensitic phase transformation. On the other hand, when Al_2O_3 is added with YSZ for coating, the temperature rise may force the aluminium atoms to diffuse into t'-ZrO_2 for stabilizing them by the formation of solid solution of YSZ-Al_2O_3 thus reducing the pace of martensitic phase transformation.

In defence and war fields, while infantry troops are fighting with enemies in the operational area, they need to fire continuously by using the weapons like 7.62 mm self-loading rifle, 5.56 mm Insas rifle and Light Machine Gun (LMG). During continuous firing of these weapons, enormous heat is released from the gun barrels to the area of lower hand guard band. Hence, the soldiers were unable to hold the hand guard during the continuous firing. In order to increase the time of firing and reduce the heat transfer to the lower hand guard band, TBCs could be provided on the surface of lower hand guard band. The gun barrel is generally made up of EN8 steel and it possesses strength of 100,000 psi (689.5 kPa) to bear gas force at the time of firing round. It possessed a Rockwell hardness of 25 to 32 HRC to withstand pressure required for propelling the firing rounds [3].

Xuemei Song et al. (2017) studied the performance of YSZ and YSZ-Al_2O_3 coating made on stainless steel in terms of thermal insulation. It is found that YSZ-Al_2O_3 coating was more stable than individual YSZ coating. The performance of coatings enhanced with increase in temperature up to 1200 °C [4]. On high temperature treatment, Y was partially removed from YSZ coating which resulted in decreased stabilization whereas on YSZ-Al_2O_3 coating removal of Y was backed up by Al diffusion thereby forming YSZ-Al_2O_3 solid solution [5,6]. Delon et al. (2018) investigated on the influence of YSZ fibres on sol-gel coating. It was observed that 60–80% YSZ fibres reinforced in the Sol-gel increased the lifetime of the components. Microstructural examination revealed that fibrous YSZ were homogeneously dispersed and were highly adherent to the powder matrix [7]. Baiamonte et al. (2015) studied the properties of micro structured and nanostructured YSZ coating and stated that micro structured plasma sprayed YSZ coating experienced a high densification at higher temperatures. Characterization results showed that nanostructured plasma sprayed YSZ preserved their porosity at high temperature and both the coating has not suffered any phase transformation at higher temperatures [8]. Mohsen Saremi et al. (2016) developed YSZ and functionally graded (FG) YSZ–Al_2O_3 TBCs by using material laminates through Atmospheric Plasma Spraying (APS). Scanning Electron Microscopic (SEM) examination showed the nanostructure in the coatings and thickness of Thermally Grown Oxide (TGO) for FG YSZ–Al_2O_3 laminates was lesser when compared with YSZ coating. It was stated that YSZ–Al_2O_3 laminate coating had higher oxidation resistance than YSZ coating [9]. Escarraga et al. (2018) developed eight YSZ/Al_2O_3 multi-layer coatings on AISI 304 stainless steel and investigated its thermal cyclic response. It was observed that iron oxides were formed in the uncoated substrates and the high-temperature oxidation intensity of

Table 1 – Temperature measurement after rifle firing.

Number of rounds fired	Supplier 1 (Temperature in °C)	Supplier 2 (Temperature in °C)
30	200	215
60	230	240
90	270	280
120	325	330
150	330	350
180	370	380

Table 2 – Chemical composition of steel materials used.

Element	EN 8 % Composition	EN 19 % Composition	EN 24 % Composition	EN 36C % Composition
Carbon	0.45	0.41	0.43	0.17
Silicon	0.19	0.23	0.27	0.25
Manganese	0.79	0.74	0.52	0.47
Chromium	0.007	1.01	1.17	0.98
Molybdenum	0.002	0.22	0.23	0.17
Nickel	0.009	0	1.37	3.33
Phosphorous	0.026	0.021	0.018	0.025
Sulphur	0.015	0.032	0.027	0.025

the coatings decreased considerably by increasing the bilayers [10]. Reza Ghasemi et al. (2017) examined the thermal insulation of YSZ TBC (nanostructured) on Nickel based super alloy (IN-738LC) and compared it with conventional YSZ TBCs. It was observed that nanostructured YSZ coating has bimodal microstructure comprising of nano sized particles and micro columnar grains [11]. Kirbiyik et al. (2017) produced double layered FG CYSZ/Al_2O_3 ceramic TBCs through HVOF and APS processes. It was observed that thermal conductivity of FG CYSZ/Al_2O_3 with 8 layers was lower when compared with the double layered CYSZ/Al_2O_3 and single layered CYSZ coatings at any temperature [12].

From the literature study, it could be witnessed that different coatings were tried for various applications but only limited works were available with functionally graded YSZ and Al_2O_3 TBCs for defense related fields like gun barrel applications. Hence in the present study, various EN grade steel materials were chosen as substrate material as they are used for making of gun barrels. Functionally graded YSZ and Al_2O_3 TBCs were developed in the weight ratio of 75:25 (YSZ:Al_2O_3) and 50:50 on the EN substrates for thermal insulation. Chemical composition, microstructural examination and strength of the coated specimens were carried out by XRD, FESEM, Energy Dispersive Spectroscopy (EDS), Thermal analysis, surface roughness test, scratch test and wear test. It was expected that YSZ and Al_2O_3 functionally graded TBCs over the EN steel substrates will aid in enhancing the thermal insulation performance of the coated material.

Material selection

In order to identify the temperature values at the time of firing of an AK47 type rifle whose gun barrel is made of EN grade steel, firing rounds were conducted in the rifle with cylindrical barrel of size 7.62 mm diameter × 39 mm length. Two different gun barrels supplied by two different manufacturers were taken for analysis. 180 rounds were fired and the temperature was measured after the completion of every 30 rounds using a thermal imaging camera. It was found that there is a steady increase in temperature while firing the rifles supplied by both the manufacturers. Values of temperature obtained during firing are listed in Table 1.

Therefore, the aim of this study is to overcome the existing problem of heat developed in gun barrel during firing operation by means of coating over the substrate. The potential gun barrel materials were chosen as EN8, EN19, EN24, EN36C and FG YSZ-Al_2O_3 in the weight ratio of 75:25 and 50:50 were used as coating materials. Selection of EN8 was based on its common usage in many mechanical elements and its wide usage for making small arms and military weapons. This alloy possesses good tensile strength, wear resistance and toughness. EN19 was preferred due to its high tensile strength, better ductility, high shock resistance and good wear resistance. It is utilized for making of engine gear boxes. EN24 was selected since it has wide range of applications in various machine elements such as gears, bolts and shafts. It has a hardness of 248–302 HBN. EN36C was a nickel chromium steel and is commonly used in making of cams and rollers [13–17]. The chemical composition of the used EN steels has been determined through Optical Emission Spectrometer (OES) and are displayed in Table 2.

Al_2O_3 (0.12% of SiO_2, 0.15% of FeO and remaining Al,) and YSZ (7.88% of Y, 0.42% of TiO_2, FeO and SiO_2 and remaining ZrO_2) were preferred for development of TBCs over the EN substrates and the standard properties of these particles are given

Table 3 – Properties of Al_2O_3 and YSZ powders. [2,18].

Property	Al_2O_3	YSZ
Density (g/cm^3)	3.69	6.02
Hardness (HV)	1175	1250
Elastic Modulus (GPa)	300	205
Thermal conductivity (W/m-K)	1.8	2.50
Compressive strength (MPa)	2100	2500
Melting point (°C)	2072	2600

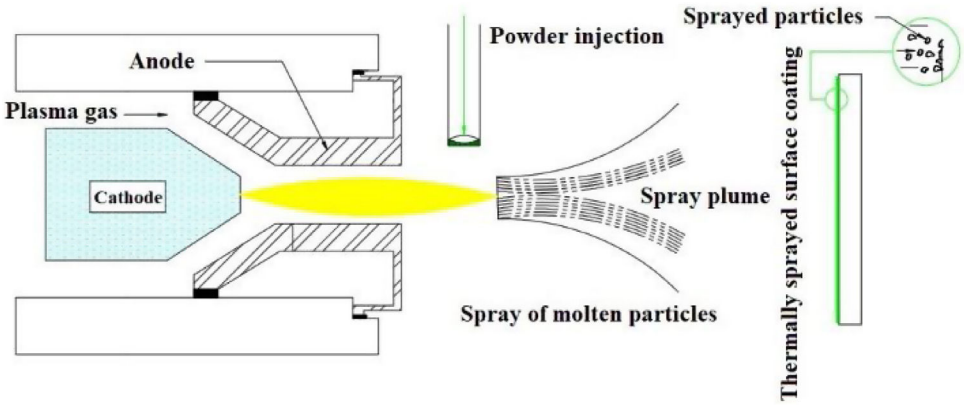

Fig. 1 – Schematic illustrations of air plasma spray deposition process.

Table 4 – Coating parameters for YSZ and Al_2O_3.

Substrate/base metal	Bond coat/thickness	Top coat/thickness	Voltage (volts)	Current (amps)	Carrier gas (Ar) flow rate (scfh)
EN 8	Ni-Cr alloy/50 μm	YSZ-Al_2O_3 200 μm	65–70	500	3 & 4
EN 19	Ni-Cr alloy/50 μm	YSZ-Al_2O_3 200 μm	65–70	500	3 & 4
EN 24	Ni-Cr alloy/50 μm	YSZ-Al_2O_3 200 μm	65–70	500	3 & 4
EN 36C	Ni-Cr alloy/50 μm	YSZ-Al_2O_3 200 μm	65–70	500	3 & 4

in Table 3. Al_2O_3 was preferred due to its high strength and stiffness when compared with other oxide ceramic materials and also possesses better dielectric properties, appreciable hardness, good thermal properties and refractoriness [2,18]. YSZ was selected due to its high strength and corrosion resistance. It is widely used in the coatings, fibre optic ferrules, wear parts, solid oxide fuel cells (SOFC) and oxygen sensors.

Experimental procedure

Steels specimens (EN 8, EN 19, EN 24, and EN 36C) with dimensions as 65 mm diameter and 5 mm thickness were used for the APS process. Nickel chrome powders (10–40 μm average particle size) were used to provide a bond coat of thickness 50 μm on the surface of the specimens. The bond coat has the chemical composition of 9.17% of Aluminium, 22.01% of Chromium, 1.08% of Yttrium and the remaining being Nickel. The bond coating is allowed to dry for 5–10 min prior to APS process. Then the specimen is mounted inside the coating chamber for the process initiation. The FG microsized YSZ (Avg. particle size 30–70 μm) and Al_2O_3 (Avg. particle size 10–30 μm) powders in weight proportions of 75:25 and 50:50 were used as coatings materials. Plasma Spray Sulzer Metco machine (12e gun model) equipped with 3 MBH Plasma spray Gun was used for producing the coating. The flame was supplied to the chamber using Argon trigger at pressure of 100 to 120 psi and maximum flow rate could be maintained as 100 scfh. In the current experiment, the carrier gas flow rate in argon trigger was kept at two different flow rates of 3 and 4 scfh. The ceramic powder mixture was then injected into a very high temperature plasma flame towards the substrate through the nozzle at the flow rate of 40 to 45 $g.min^{-1}$ by keeping the flow distance of 2 to 3 inches. This results in rapid heating of the ceramic powders and consequently the molten ceramic powders were accelerated at high velocity towards the substrate surface. When the powders come into contact with the substrate, upon rapid cooling, coating was applied over the surface. The FG YSZ-Al_2O_3 ceramic powder coating of thickness 200 microns were top coated on the EN series steels separately with weight proportions 75:25 and 50:50 and the properties of coated specimens were investigated in detail. The schematic illustration of the APS process is shown in Fig. 1. The coating parameters used for development of TBCs are given in Table 4.

Fig. 2(a) and (b) depicts the schematic representation of bond coat and top coat over the steel substrates using Ni-Al alloy and FG YSZ-Al_2O_3 (in two different weight proportions). Such coated specimens were expected to possess high temperature stability and hence their thermal insulation performance Fig. 2.

Fig. 3 shows the thermal testing apparatus which was used to find the surface temperature of the uncoated and FG ceramic powder coated specimens. Heat was supplied to the surface opposite to the exposed surface through an induction heater and was maintained at a constant temperature of 200 °C. Thermocouple was used in conjunction with the heater to find out the surface temperature. IR Thermometer was used to confirm the temperature measurement obtained in the thermal testing apparatus. It is non-contact temperature estimation gadget which identify the infrared vitality radiated, transmitted or reflected and converts into temperature perusing or thermogram. The process was carried out on the sample for 20 min and the temperature was noted at various time intervals. Uncoated steel substrates and FG YSZ-Al_2O_3 coated steel substrates were then subjected to thermal

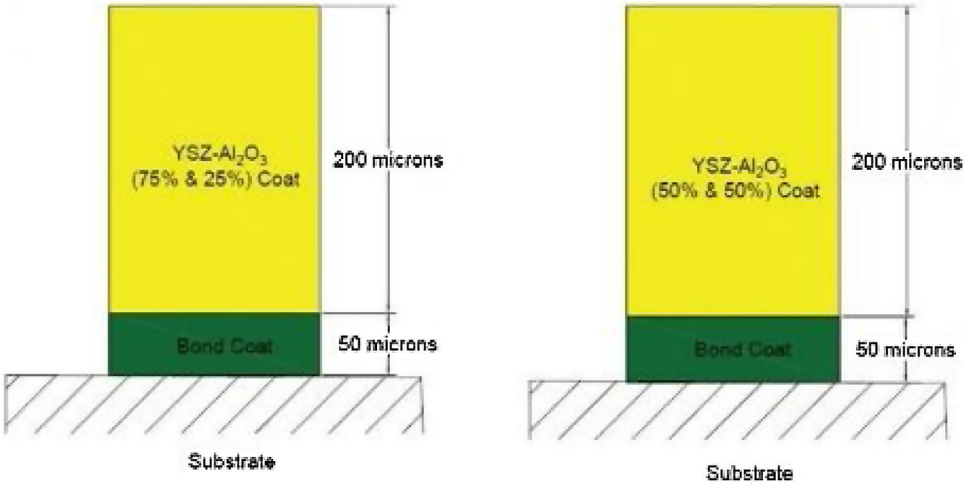

Fig. 2 – Schematic illustration of coatings of YSZ-Al_2O_3 (a) 75:25, (b) 50:50.

Fig. 3 – Thermal testing apparatus.

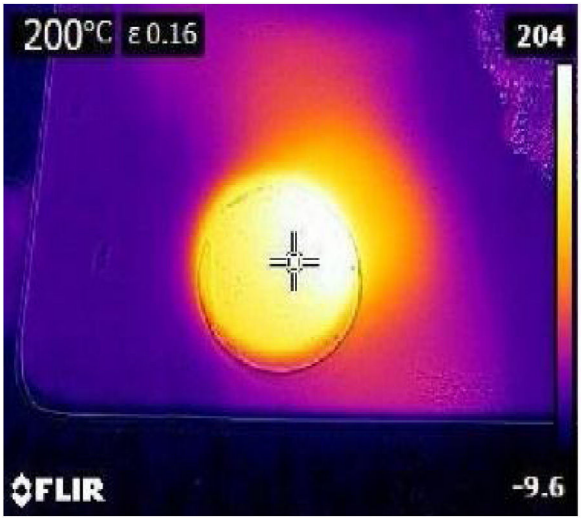

Fig. 4 – Thermal image of the coated substrate.

testing process. The obtained thermal image of the coated specimen is shown in Fig. 4.

All FG YSZ-Al_2O_3 coated specimens (with weight proportions 75:25 and 50:50) manufactured through two different carrier gas concentrations of 3 and 4 scfh were subjected to wear and scratch tests. Wear test was conducted to evaluate the wear characteristics of uncoated and coated steels to determine materials adequacy for application and the effect of process parameters on the wear performance. During wear test, a pin was kept in contact against a rotating disc under sliding conditions. Experiments were carried out on a track of mean diameter 80 mm, applied weight of 20 N, speed of 50 rpm and for the time of 15 min. In addition to wear test, scratch test was also performed on the coated steel specimen at three different loads of 1, 2 and 3 kg after exposing the specimens to a temperature of 200 °C for 1 h.

Results and discussion

Microstructural examination

XRD analysis is performed on both the FG YSZ-Al_2O_3 coated EN steel substrate to identify the phase composition using Cu-Kα radiation (λ = 1.545 nm) and shown in Fig. 5a and b. The generator of X-ray was set at 30 mA and 45 kV and the scanning was performed for the diffraction angle 2θ varying from 5° to 90°. Both 75:25 and 50:50 FG YSZ-Al_2O_3 coated EN substrate displayed the presence of cubic tetragonal crystal structure. Similar pattern has been observed in plasma sprayed YSZ-Al_2O_3 multilayer TBCs by the early researchers [3,14]. The formation of such non-equilibrium tetragonal phase was attributed to the higher solidification rate of powders during the APS process [10]. Hence it could be ascertained that YSZ-Al_2O_3 were deposited on the EN steel substrate through the APS process due to the formation of tetragonal phase.

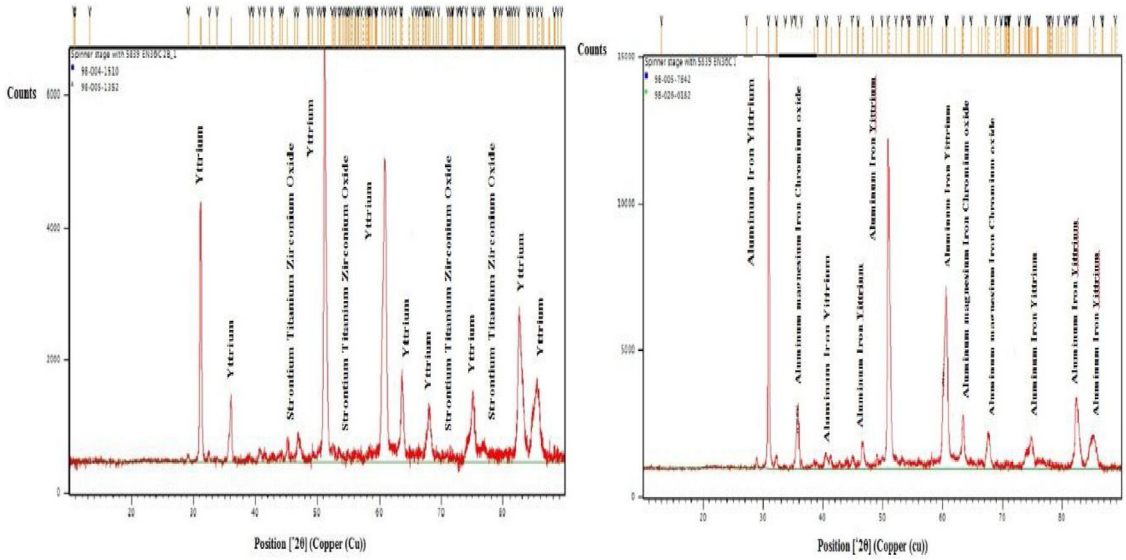

Fig. 5 – XRD pattern of YSZ-Al_2O_3 (a) 75:25, (b) 50:50.

SEM analysis was performed on the both YSZ-Al_2O_3 coated EN steel substrate to observe their surface morphology and are shown in Figs. 6 and 7. Elemental identification was assessed through the EDS attachment with SEM. As observed in figures, the top surface of both the functionally graded YSZ-Al_2O_3 coated EN steel substrate appears to be rough and contains laminar structures. Slight porosity is observed on both the coated specimen. In addition, 50:50 YSZ-Al_2O_3 appears to be much denser than the 75:25 YSZ-Al_2O_3 coatings. The coating gets denser in 50:50 YSZ-Al_2O_3 due to the increase in Al_2O_3, which has a lower melting point of 2325 K as compared to the higher melting point of YSZ which is 2950 K. Similar phenomena were also reported in case of plasma sprayed YSZ/Al_2O_3 TBCs [12]. EDS analysis on the top coat of both the functionally graded coatings ensures the presence of elements such as Zr, Al, O as observed in Figs. 6 and 7 respectively.

Fig. 8a and b depicts the SEM image EN36C steel cross section coated with YSZ-Al_2O_3 in 75:25 and 50:50 proportions which clearly reveals that significant adhesion exist between top coat, bond coat and metallic substrate. Low degree of porosity could be observed in both the FG coatings which was due to the presence of Al_2O_3 which is a stoichiometric oxide. The diffusivity of oxygen ions is lesser which results in lesser permeability. Moreover, the small particle sized Al_2O_3 powders contributed to the low porosity of both the FG ceramic coatings.

Surface roughness

Surface roughness of uncoated and coated EN 36C steel specimens was measured using A SJ-310 Mitutoyo (Japan) surface roughness tester as per the DIN EN ISO 3274 standard. The surface roughness was measured at different points on the top surface of the coat and the average value was considered finally for analysis. The obtained surface roughness values are shown in Table 5. The surface roughness of the uncoated EN 36C steel is found to be less than 6 μm whereas the surface roughness value is slightly more than 6 μm in the 75:25 YSZ-Al_2O_3 and 50:50 YSZ-Al_2O_3 coated EN 36C steel substrate. This could be attributed to the homogenous distribution of the partially molten ceramic particles on the surface of the substrate and such similar behaviour was observed in case of Ni-YSZ deposited stainless steel by few researchers [13]. Among the coated samples, 75:25 YSZ-Al_2O_3 coated EN 36C has the higher surface roughness value compared to the 50:50 YSZ-Al_2O_3 coated EN 36C. This behaviour was due to the presence of more amount YSZ particles in case of 75:25 YSZ-Al_2O_3 coating as the YSZ particles are coarser in size (30–70 μm). As there is an increase in finer Al_2O_3 particles in 50:50 YSZ-Al_2O_3 coating, a decrease in the surface roughness compared to the 75:25 YSZ-Al_2O_3 coating could be witnessed.

Thermal testing

TBCs are generally exposed to thermal cycling during their service. The coefficient of thermal expansion varies between top coat, bond coat and the metallic substrate. Hence expansion mismatch happens at the interface between these materials which will eventually result in development of thermal residual stresses. Therefore, failure of such coating will result due to spallation or debonding when exposed to a higher temperature [14]. Based on this, thermal testing was carried out using thermal imager for the coated specimens produced with carrier gas concentrations of 3 scfh and 4 scfh and the observed temperature values are plotted as shown in Figs. 9 and 10.

It could be observed from Fig. 9 that the surface temperature increases with increase in the exposure time for both uncoated and FG ceramic coated steels. The temperature on the surface of uncoated EN steels increases rapidly when compared to the YSZ-Al_2O_3 coated steels. Among the coated steels, the 75:25 YSZ-Al_2O_3 coated steels has better insulation performance than the 50:50 YSZ-Al_2O_3 coated steels. It is observed that a lowest surface temperature of 141.5 °C is observed in 75:25 YSZ-Al_2O_3 coated EN36C steels for the maximum exposure time of 20 min whereas the highest

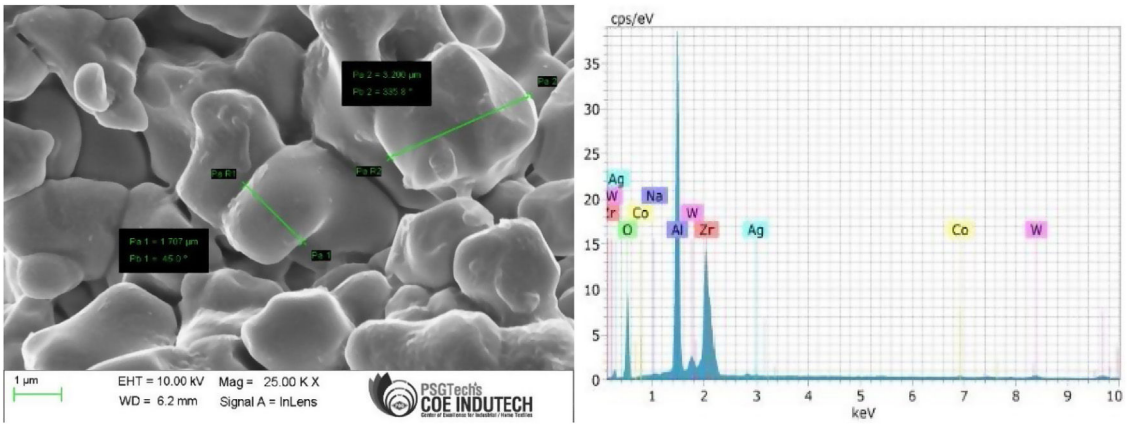

Fig. 6 – SEM and EDS of 75:25 YSZ-Al_2O_3 deposited steel substrate.

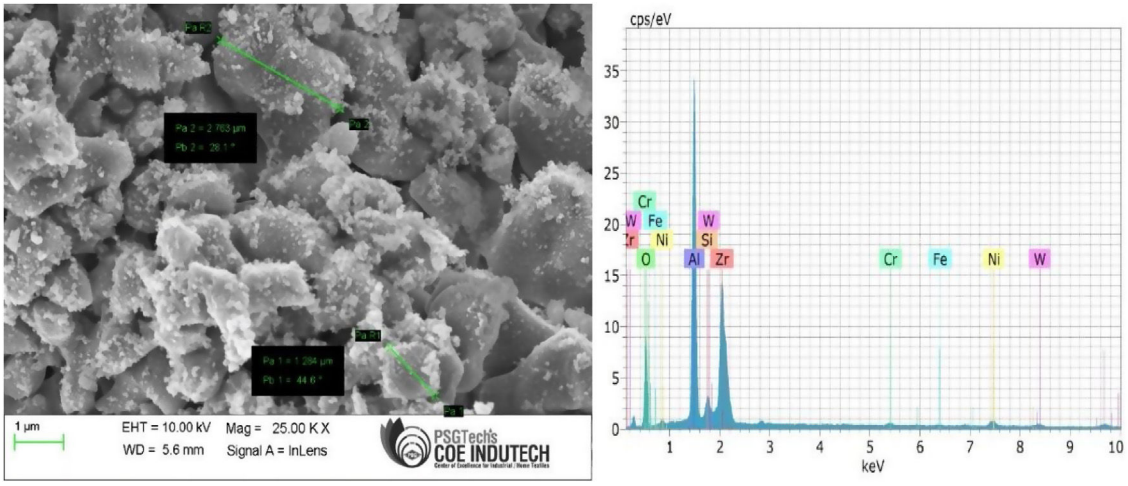

Fig. 7 – SEM and EDS of 50:50 YSZ-Al_2O_3 deposited steel substrate.

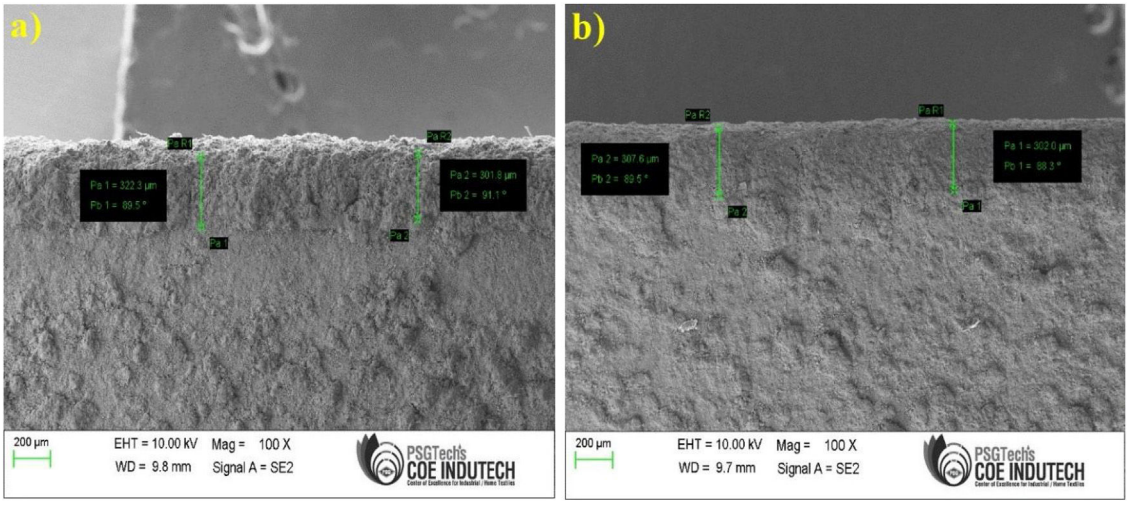

Fig. 8 – Cross section of the YSZ-Al_2O_3 (a) 75:25, (b) 50:50.

Table 5 – Surface roughness of the uncoated and coated EN substrate.

S.NO	Material	Avg. surface roughness (Ra) μm
1	EN 8 Uncoated	4.53 ± 0.09
2	EN 19 Uncoated	5.45 ± 0.21
3	EN 24 Uncoated	4.55 ± 0.18
4	EN 36C Uncoated	5.71 ± 0.15
5	EN 36C coated YSZ	6.67 ± 0.05
6	EN 36C coated Al_2O_3	6.63 ± 0.05
7	EN36C coated YSZ-Al_2O_3 (50–50%)	6.25 ± 0.02
8	EN 36C coated YSZ-Al_2O_3 (75–25%)	6.31 ± 0.05

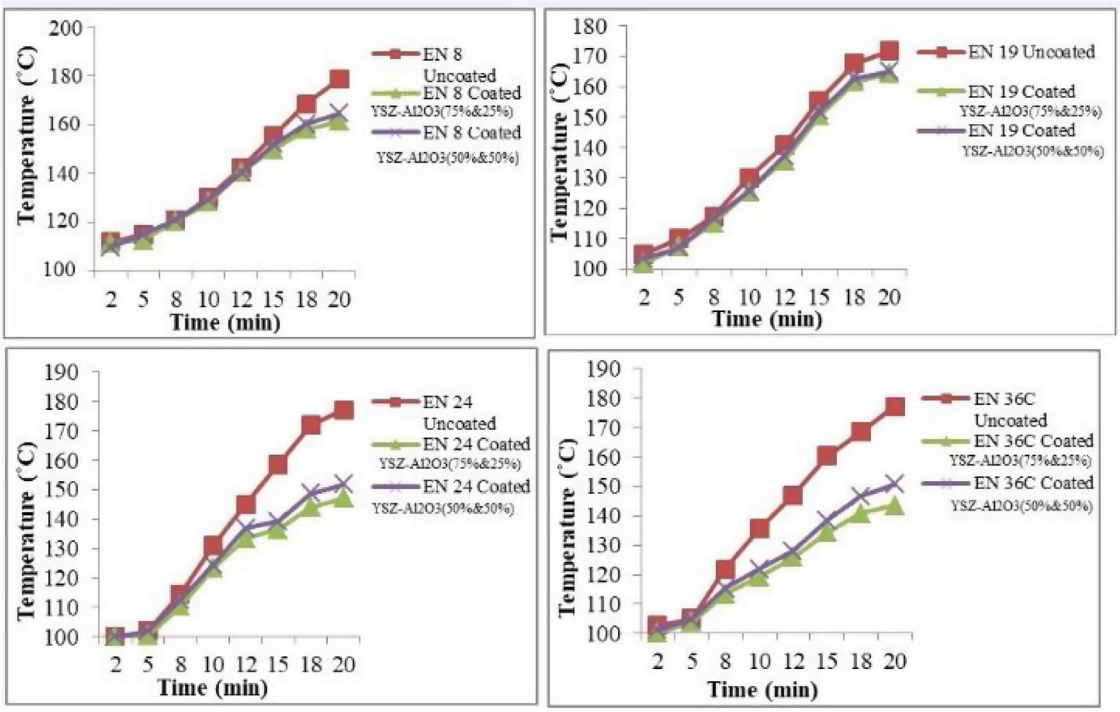

Fig. 9 – Surface temperature of the specimens (3 scfh) with respect to time.

surface temperature of 178.7 °C is observed in the uncoated EN 8 steel for the same exposure time. Fig. 10 depicts that surface temperature of both coated and uncoated steels produced under the carrier gas flow rate at 4 scfh, increases upon exposure. Among the coated steels, 75:25 YSZ-Al_2O_3 coated steels have better insulation performance than the 50:50 YSZ-Al_2O_3 coated steels. 75:25 YSZ-Al_2O_3 coated EN36C steel has shown better performance recording the lowest surface temperature (143.5 °C) for the maximum exposure time of 20 min whereas the EN 8 steel possess the highest surface temperature for the same exposure time as in the previous case. Presence of porosity in the coatings has greater significance in decreasing the thermal conductivity of the coating [15]. Similar study was reported earlier which stated that porosity in TBCs offers advantages such as increase in strain endurance and reduction in thermal conductivity [16]. The magnitude of the surface temperature was relatively higher for all the specimens produced under 4 scfh for all the exposure time compared to the specimens produced with a gas flow rate of 3 scfh. From this, it is evident that flow rate of carrier gas has greater significance over the inflight particle properties and the trajectory of the particles towards plasma jet. As the gas powder mixtures are

Table 6 – Wear test results.

Material	Wear volume rate (mm^3/N.m)	Frictional force (N)	Coefficient of friction
EN 8	1.59×10^{-6}	13	0.357
EN 19	1.69×10^{-6}	13.4	0.387
EN24	1.01×10^{-6}	13	0.450
EN 36C	1.02×10^{-6}	8.2	0.350
EN 36C (75:25 YSZ-Al_2O_3 coated)	1.85×10^{-7}	9.6	0.210
EN 36C (50:50 YSZ-Al_2O_3 coated)	2.21×10^{-7}	9.7	0.220

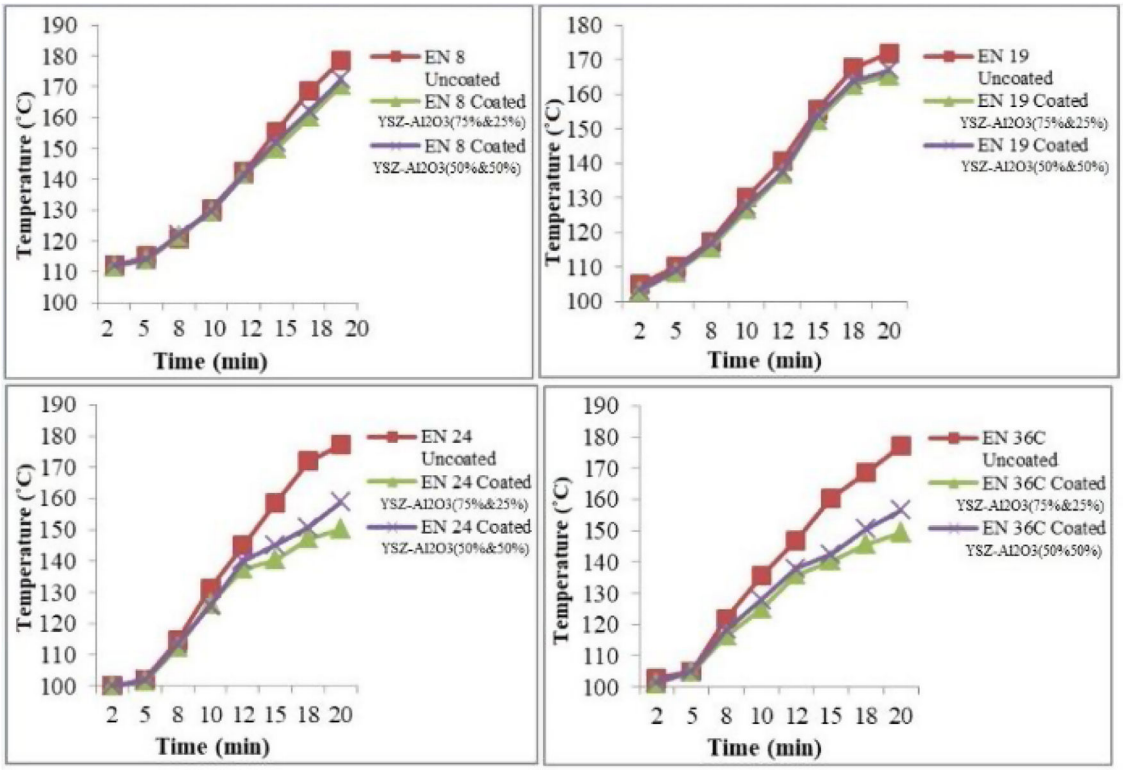

Fig. 10 – Surface temperature of the specimens (4 scfh) with respect to time.

externally injected into plasma jet, exchange of heat between cold particles and the hot plasma jet affects the temperature circulation between the plasma jet and the ceramic particles.

In addition, parameters such as torch power, composition of the gas, diameter of the nozzle and momentum of particle also affects the interaction of the particles with the plasma jet. Among these, carrier gas flow rate mainly affects momentum of the particles. As the momentum varies from between low and high in three stages, the particle to be coated may bounce away from plasma flow after which it penetrates into plasma jet. When the particle had entered into the plasma jet, it may enter and cross over the jet or it may continue to flow along with the jet. Thus the variation in flow rate of carrier gas would modify the particle trajectory below or above the plasma jet axis. From the thermal performance analysis of the coatings deposited under 3 and 4 scfh, it can be seen that the flow rate of 3 scfh provides the optimum particle trajectory (and better spray performance) along with a high coating particle flow density at higher temperature and velocity of the plasma jet. It could be assumed that the centre line of particle flux and plasma jet axis were coaxial at a flow rate of 3 scfh. Similar studies on variation of plasma spray parameters expressed that the carrier gas flow rate variation greatly affected the in-flight particle behaviour [17–19].

Altogether, 75:25 YSZ-Al_2O_3 coated EN 36C steel fabricated under carrier gas with a flow rate of 3 scfh had better insulation performance at a temperature of 141.5 °C compared to all other steel substrates selected for the study. More specifically, coated EN 36C steel outperformed all other coated EN steels due to the presence of higher nickel content (3.33%). In addition to strength, hardness and toughness, nickel offers corrosion and scaling resistance also at high temperatures [20–22]. In order to endorse this, macroscopic observation (Fig. 11) has been performed on the YSZ-Al_2O_3 coated EN 36C specimen (before and after coating) by exposing it to a temperature of 200 °C for the time of 20 min. It could be observed that there is no visible spallation of the coat for the input temperature of 200 °C even after the maximum exposure time of 20 min, which indicates that there is significant adhesion between top coat, bond coat and metallic substrate.

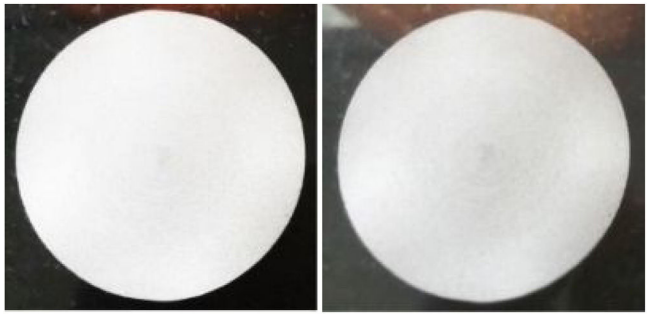

Fig. 11 – Macroscopic observation of thermal tested YSZ-Al_2O_3 deposited EN36C specimen (a) Before exposure and (b) After exposure.

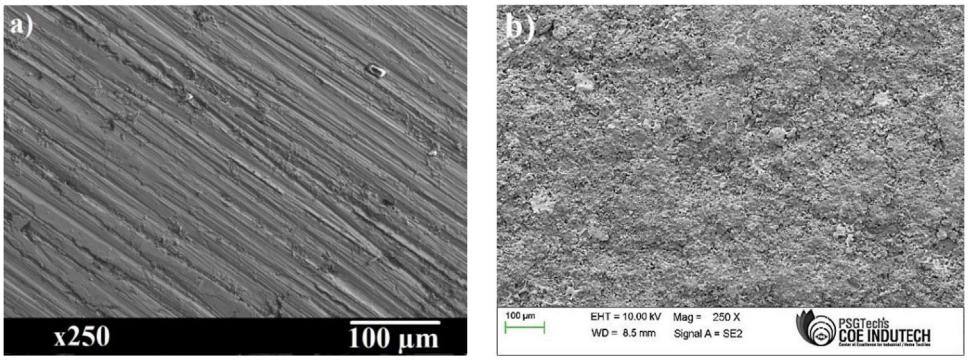

Fig. 12 – SEM micrographs of worn out surfaces: (a) EN 8 steel (b) YSZ-Al_2O_3 coated EN36C steel.

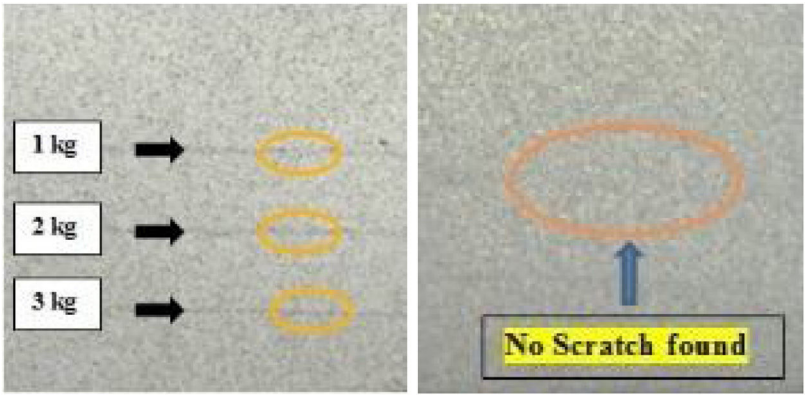

Fig. 13 – Macroscopic examination of scratch tested (a) 50:50 YSZ-Al_2O_3 (b) 75:25 YSZ-Al_2O_3 deposited EN36C steel.

Wear and scratch test

The obtained wear test results are shown in Table 6. The lowest wear rate and lowest coefficient of friction was obtained for 75:25 YSZ-Al_2O_3 coated EN 36C steel specimen compared to all other materials. This could be attributed to the better intersplat bonding and higher micro-hardness of YSZ (1250 HV) and due to the presence of higher weight fractions of YSZ in 75:25 YSZ-Al_2O_3 coating. On the other hand, highest wear rate was observed for the uncoated EN 8 steel substrate.

SEM analysis of the worn surface of the uncoated EN 8 steel and 75:25 YSZ-Al_2O_3 coated EN 36C steel are shown in Fig. 12(a) and (b) respectively. In uncoated EN8 steel, the wear tracks are more prominent with the existence of parallel ploughs and deep continuous grooves in rotary direction evidencing adhesive and abrasive wear. The worn out surface of the 75:25 YSZ-Al_2O_3 coated EN 36C steel revealed lesser deformation with less number of prominent wear tracks. However, surface is characterized with micro cracks, grooves, plowing marks and darker zone at several places. This is evident that material removal from the coating has happened through abrasive wear phenomenon, which was also reported consistently by several researchers [23–25]. The darker zones on the surface may represent the formation of fine debris compaction during the wear test and similar behaviour was reported earlier also [26]. Generally, the failure of thermal sprayed ceramic coating occurs through three processes as stated by Hawthorne et al. such as microchipping and plowing, splat boundaries debonding and splat boundary fracture [27]. In case of poor bonding between splats, major material removal occurs as a result of splat boundary debonding which consequently end up in high material removal and high wear rate. However, lowest wear rate is obtained for 75:25 YSZ-Al_2O_3 coated EN 36C steel which is evident that there exists a greater cohesion between the splat boundaries which in turn enhanced the wear resistance of the material. Since the 75:25 YSZ-Al_2O_3 coated EN 36C steel has outperformed in the metallurgical analysis and wear tests, the coated specimens were alone subjected to scratch testing.

The scratch resistance of the both 75:25 YSZ-Al_2O_3 and 50:50 YSZ-Al_2O_3 coated EN 36C specimen was tested by applying different loads using scratch tester and the scratch tracks recorded are shown in Fig. 13. It is inferred that upon scratching at different loads, the coating has not been damaged and the base metallic substrate was not exposed to scratch loads. At a low load of 1 kg, the groove of scratch is shallow with a narrow width. As the load was increased to 2 kg, fewer cracks with slight deformation could be observed on the scratch edges. Further increase in the applied load to 3 kg led to a slight increase in depth and width of the scratch groove for 50:50 YSZ-Al_2O_3 coated steel specimen but the coating has not been damaged and the base metallic substrate was not exposed. In general, during scratch testing the indenter tip generates shear stress concentration on the contact surface causing a noticeable deformation near the tip. To release this energy and affluence the free energy of the coating, microsized radial and

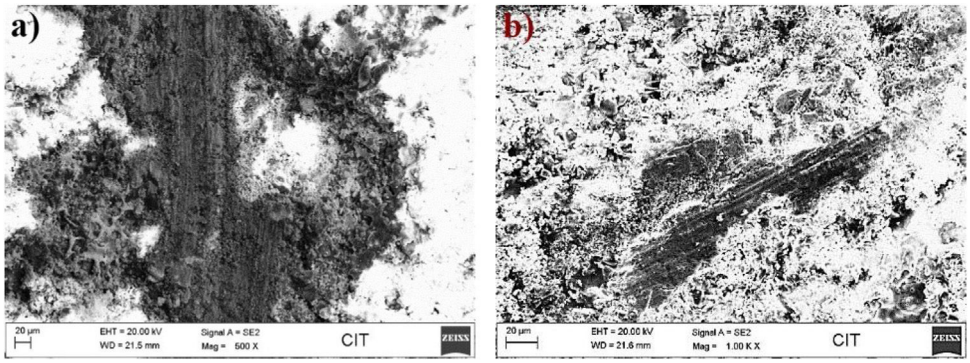

Fig. 14 – SEM micrographs of scratch tested (a) 50:50 YSZ-Al_2O_3 (b) 75:25 YSZ-Al_2O_3 deposited EN36C steel.

lateral cracks are instigated by core defects. This phenomenon could be noticed for 50:50 YSZ-Al_2O_3 coated steel specimen and this slight increase in deformation could be attributed to the presence of minute pores and partially melted YSZ particles in the coating and the similar phenomenon was reported in earlier studies [28,29]. In the 75:25 YSZ-Al_2O_3 coated EN 36C specimen surface as shown in Fig. 13(b), such scratches and deformation could be sparsely observed. Hence, 75:25 YSZ-Al_2O_3 offers better scratch resistance even at higher load which could be possibly attributed to the presence of higher quantity of YSZ which has an appreciable hardness of 1250 HV and this offered resistance to scratch at all the loads. SEM micrographs of both YSZ-Al_2O_3 coatings substantiates the above statements and are shown in Fig. 14a and b.

Conclusion

TBCs were applied on the four different steel substrates using FG YSZ-Al_2O_3 ceramic materials in the weight proportion of 75:25 and 50:50 using APS process with two different carrier gas concentrations such as 3 and 4 scfh successfully. These coated and uncoated specimens were subjected to thermal, wear and scratch tests along with morphological characterization and the following results were obtained:

- From XRD, it was concluded that 75:25 and 50:50 YSZ-Al_2O_3 deposited EN substrate reveal the presence of cubic tetragonal structure. SEM images revealed that the coatings were devoid of porosity and were densely packed on the top of bond coat.
- From surface roughness tests it was observed that, 50:50 YSZ-Al_2O_3 coated EN 36C material has higher surface roughness of $6.25 \pm 0.02\ \mu m$ when compared all other coated and uncoated steels. Yet the surface roughness value of 75:25 YSZ-Al_2O_3 was only marginally higher ($6.31 \pm 0.05\ \mu m$) than 50:50 YSZ-Al_2O_3 coated EN 36C steel.
- Thermal tests on 75:25 YSZ-Al_2O_3 coated EN 36C steel fabricated under carrier gas flow rate of 3scfh showed better insulation performance without any visual spallation, compared to all other steels.
- Wear and scratch tests revealed that 75:25 YSZ-Al_2O_3 coated EN 36C steel has better wear and scratch resistance compared to other materials selected for study. Overall, from the study it could be concluded that the lower guard hand of the AK47 rifle could be coated with 75:25 FG YSZ-Al_2O_3 in order to reduce the heat transfer at the time of firing rounds.

REFERENCES

[1] Liu, Bin, Y. Liu, C. Zhu, H. Xiang, H. Chen, L. Sun, Y. Gao, Y. Zhou, Advances on strategies for searching for next generation thermal barrier coating materials, J. Mater. Sci. Technol. 35 (5) (2019) 833–851.
[2] L. Rajesh kumar, K.S. Amirthagadeswaran, Corrosion and wear behaviour of nano Al2O3 reinforced copper metal matrix composites synthesized by high energy ball milling, Part. Sci. Technol. 38 (2) (2020) 228–235, http://dx.doi.org/10.1080/02726351.2018.1526834.
[3] M. Ramesh, K. Marimuthu, Microstructural, thermal and wear behavior of YSZ/Al_2O_3 thermal barrier coatings for gun barrel applications, Digest. J. Nanomater. Biostruct. 15 (2) (2020) 527–536.
[4] X. Song, Z. Liu, M. Kong, C. Lin, L. Huang, X. Zheng, Thermal stability of yttria-stablized zirconia (YSZ) and YSZ-Al2O3 coatings, Ceram. Int. 43 (2017) 14321–14325.
[5] Z.E. Sanchez-Hernandezm, M.A. Dominguez-Crespo, A.M. Torres-Huerta, E. Onofre-Bustamante, J. Andraca Adame, H. Dorantes-Rosales, Improvement of adhesion and barriers properties of biomedical stainless steel by deposition of YSZ coatings using RF magnetron sputtering, Eur. J. Mater. Charact. 91 (2014) 892.
[6] B. Bernard, A. Quet, L. Bianchi, A. Joulia, A. Malie, V. Schik, B. Remy, Thermal insulation properties of YSZ coatings: suspension plasma spraying (SPS) versus electron beam physical vapor deposition (EB-PVD) and atmospheric plasma spraying (APS), Adv. Mater. Sci. 318 (2017) 122–128.
[7] E. Delon, F. Ansart, Duluard, J.P. Bonino, Monceau, A. Rouaix, R. Mainguy, C. Thouron, A. Malie, A. Joulia, L. Bianchi, P. Gomez, Outstanding durability of solo gel thermal barrier coatings reinforced by YSZ, Eur. J. Ceram. 38 (14) (2018) 4719–4731.
[8] L. Baiamonte, F. Marra, G. Pulci, J. Tirillo, F. Sarasini, C. Bartuli, T. Valente, High temperature mechanical characterization of plasma-sprayed zirconia-yttria from conventional and nanostructured powders, Surf. Coat. Technol. 277 (2015) 289–298.
[9] M. Saremi, Z. Valefi, Thermal and mechanical properties of nano-YSZ–Alumina functionally graded coatings deposited by nano-agglomerated powder plasma spraying, Ceram. Int. 40 (2016) 13453–13459.

[10] A. Escarraga, A. Toro, Y. Aguilar, Julio Caicedo., Thermal cyclic response of [8YSZ/Al2O3] n multilayered coatings deposited onto AISI 304 stainless steel, Mater. Chem. Phys. 216 (2018) 526–533.
[11] R. Ghasemi, H. Vakilifard, Plasma-sprayed nanostructured YSZ thermal barrier coatings: thermal insulation capability and adhesion strength, Ceram. Int. 43 (12) (2017) 8556–8563.
[12] F. Kirbiyik, M.G. Gok, G. Goller, Microstructural, mechanical and thermal properties of Al2O3/CYSZ functionally graded thermal barrier coatings, Surf. Coat. Technol. 329 (2017) 193–201.
[13] P.C. Tsai, P.S. Hsu, High temperature corrosion resistance and microstructural evaluation of laser-glazed plasma-sprayed zirconia/MCrAlY thermal barrier coatings, Surf. Coat. Technol. 183 (2004) 29–34.
[14] M.S. Ahmadi, R. Shoja-Razavi, Z. Valefi, H. Jamali, The effect of laser surface treatment on the thermal shock behavior of plasma sprayed Al2O3/YSZ multilayer thermal barrier coatings, Surf. Coat. Technol. 366 (2019) 62–69.
[15] U. Saral, N. Toplan, Thermal cycle properties of plasma sprayed YSZ/Al2O3 thermal barrier coatings, J. Surf. Eng. 25 (2009) 541–547.
[16] G. Prasad, R.P.S. Chakradhar, M. Srivastava, Development and characterization of Ni-YSZ coating on stainless steel by HVOF Process, Int. J. Eng. Res. Technol. 6 (2017) 263–266.
[17] T.J. Lu, J.W. Hutchinson, Thermal conductivity and expansion of cross-ply composites with matrix cracks, J. Mech. Phys. Solids 43 (1995) 1175–1198.
[18] V. Kumar, B. Kandasubramanian, Processing and design methodologies for advanced and novel thermal barrier coatings for engineering applications, Particuology 27 (2016) 1–28.
[19] A.G. Evans, D.R. Mumm, J.W. Hutchinson, G.H. Meier, F.S. Pettit, Mechanisms controlling the durability of thermal barrier coatings, J. Surf. Eng. Mater. Adv. Technol. 46 (2001) 505–553.
[20] A. Kucuk, Rogerio, S. Lima, C. Christopher Berndt, Influence of plasma spray parameters on in-flight characteristics of ZrO2-8 wt% Y2O3 ceramic particles, J. Am. Ceram. Soc. 84 (2001) 685–692.
[21] W. Zhang, L.L. Zheng, H. Zhang, S. Sampath, Study of injection angle and carrier gas flow rate effects on particles in-flight characteristics in plasma spray process: modeling and experiments, Plasma Chem. Plasma Process. 27 (2007) 701–716.
[22] C.S. Ramachandran, V. Balasubramanian, P.V. Ananthapadmanabhan, Multiobjective optimization of atmospheric plasma spray process parameters to deposit yttria-stabilized zirconia coatings using response surface methodology, J. Therm. Spray Technol. 20 (3) (2011) 590–607.
[23] P. Psyllaki, M. Jeandin, D.I. Pantelis, Microstructure and wear mechanisms of thermal sprayed alumina coatings, Mater. Lett. 47 (2001) 77–82.
[24] Z. Yin, S. Tao, X. Zhou, C. Ding, Tribological properties of plasma sprayed Al/Al2O3 composite coatings, Wear 263 (2007) 1430–1437.
[25] G. Perumal, M. Geetha, R. Asokamani, N. Alagumurthi, Wear studies on plasma sprayed Al2O3-40 wt% 8YSZ composite ceramic coating on Ti–6Al–4V alloy used for biomedical applications, Wear 311 (2014) 101–113.
[26] C. Lamuta, G. DiGirolamo, L. Pagnotta, Microstructural, mechanical and tribological properties of nanostructured YSZ coatings produced with different APS process parameters, Ceram. Int. 41 (2015) 8904–8914.
[27] H. Hawthorne, L. Erickson, D. Ross, H. Tai, T. Troczynski, The microstructural dependence of wear and indentation behaviour of some plasma-sprayed alumina coatings, Wear 203–204 (1997) 709–714, http://dx.doi.org/10.1016/s0043-1648(96)07399-1.
[28] S. Sathish, M. Geetha, R. Asokamani, Comparative studies on the corrosion and scratchbehaviors of plasma sprayed ZrO2 and WC-Co coatings, Proc. Mater. Sci. 6 (2014) 1489–1494, http://dx.doi.org/10.1016/j.mspro.2014.07.128.
[29] L. Rajeshkumar, K.S. Amirthagadeswaran, Variations in the properties of copper-alumina nanocomposites synthesized by mechanical alloying, Mater. Tehnol. 59 (1) (2019) 57–63.